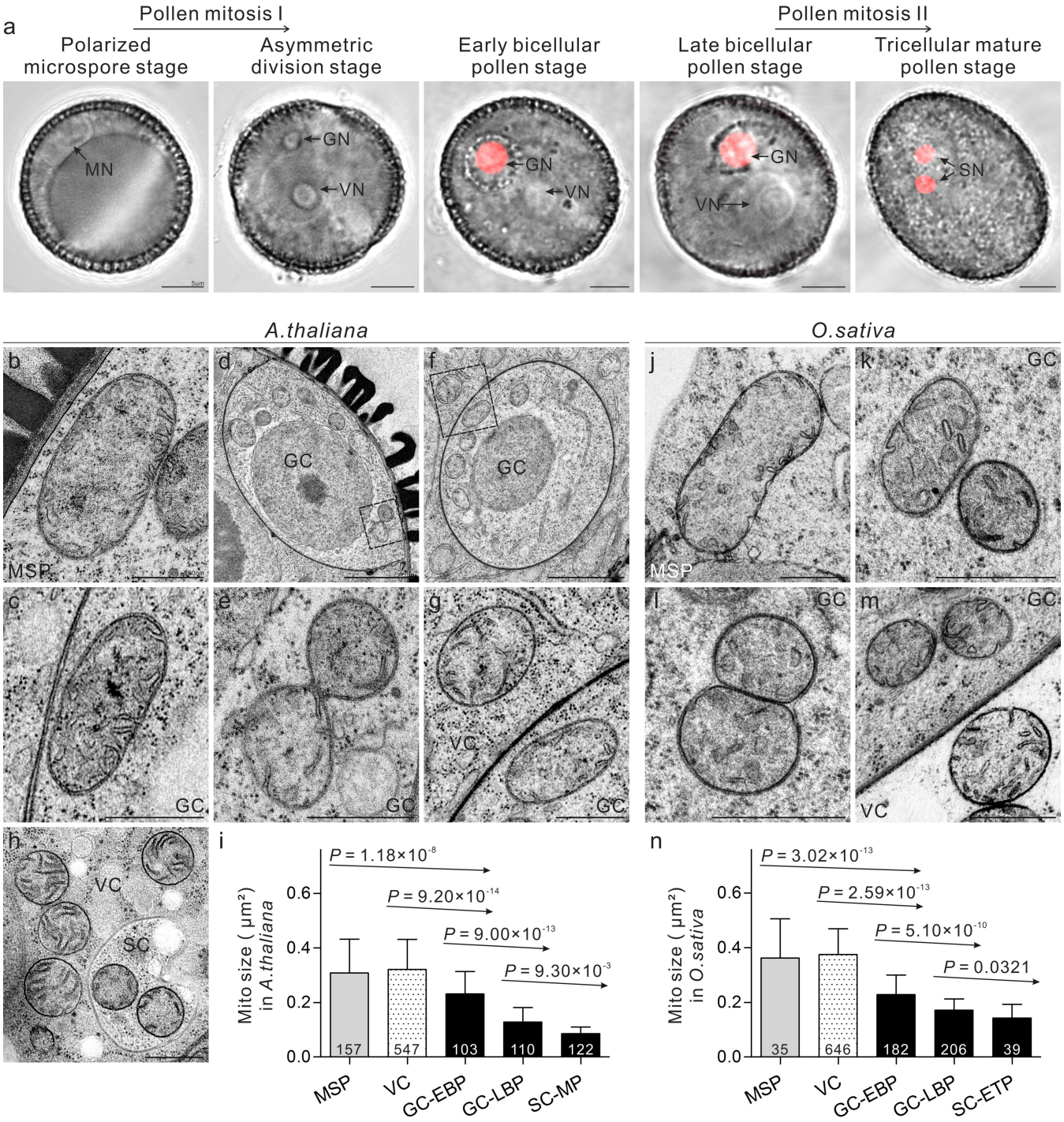

Extended Data Fig. 1 | The fission of paternal mitochondria during male gametogenesis.

a, The male gametogenesis process in the *A. thaliana ProHTR10: HTR10-RFP* line. The microspore (MSP) undergoes an asymmetrical division (pollen mitosis I) to form a larger VC and a smaller GC. VC exits the cell cycle, but GC completes pollen mitosis II (a symmetrical division) to produce two SCs. GC and SCs are collectively named as male germline cells. Thus, the male gametophyte (pollen) is a simplified plant body containing only two cell lineages, the VC wraps around the germline cells to form a "cell(s) within a cell" structure. **b-i**, Paternal mitochondrial dynamic during male gametogenesis in *A. thaliana*. Mitochondrial morphology in microspore (**b**) . Paternal mitochondrial morphology in the GC right after asymmetric microspore division (**c-e**) . The paternal mitochondria in GC, which were inherited from microspore after asymmetric microspore division and then rapidly divided into the smaller mitochondria. With the formation of SC, paternal mitochondria in GC (**f**, **g**) and SC (**h**) were significantly smaller than their counterparts in VC. **j-n**, Paternal mitochondrial dynamic during male gametogenesis in *O. sativa*. Mitochondrial morphology in rice microspore(**j**). Paternal mitochondrial morphology in rice GC (**k-m**) . The paternal mitochondria in GC, which were

inherited from microspore after asymmetric microspore division and then also rapidly divided into the smaller mitochondria. The statistics of mitochondrial size during male gametogenesis of *A. thaliana* (**i**) and *O. sativa* (**n**). Results are from three independent experiments. Statistical number of mitochondria in *A. thaliana* and *O. sativa* are put in the base of data bars. Statistical significance is determined by one-way ANOVA ($P < 0.05$, *; $P < 0.001$, ***) and the error bars show standard deviation (SD). Scale bars, 5μm (**a**), 500nm (**b, c-h**, **j-m**), 2μm (**d**, **f**). MSP, microspore; MN, microspore nucleus; GC, generative cell; GN, generative cell nucleus; SC, sperm cell; SN, sperm cell nucleus; VC, vegetative cell; VN, vegetative cell nucleus; EBP, early bicellular pollen; LBC, late bicellular pollen; ETP, early tricellular pollen; MP, mature pollen.

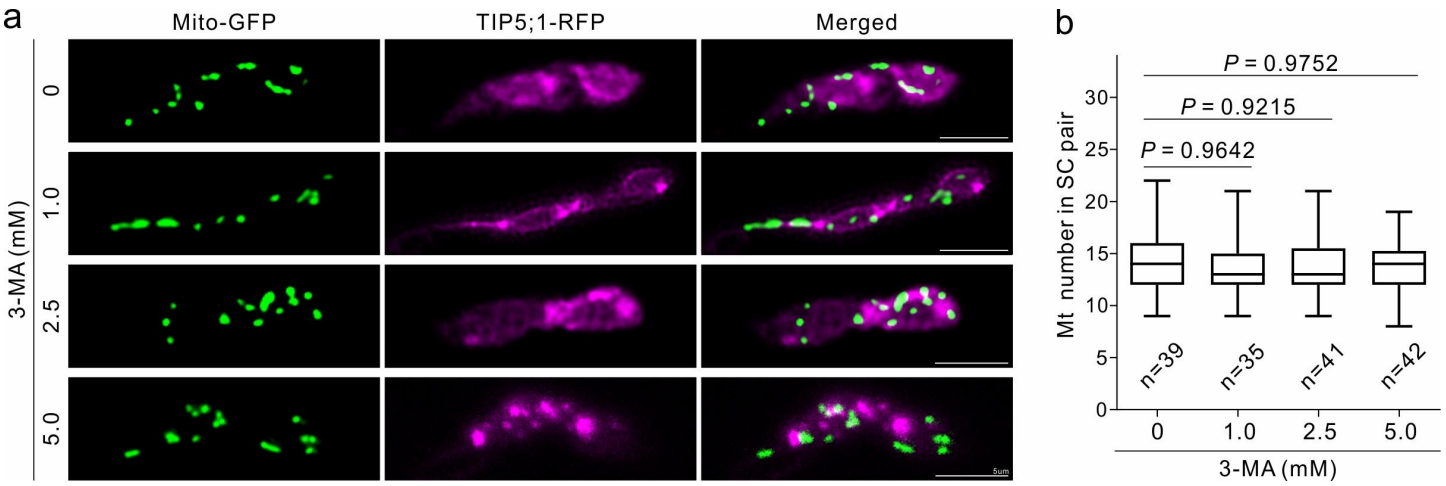

Extended Data Fig. 2 | Inhibition of autophagosome formation by 3-MA did not block PME.

a, The representative picture showed that autophagy inhibitor 3-MA could not effectively interfere with PME to cause mitochondrial accumulation. The pollen grains from a vacuole and mitochondrion double-labeled transgenic line were put into the PGM containing different concentrations of 3-MA, and the mitochondria dynamics in the SCs within germinated pollen tubes were observed after 5 hours. Scale bars, 5μm. **b**, The number statistics of mitochondria (Mt) in the SCs treated with different concentrations of 3-MA after 5 hours. Results are from three independent experiments. Statistical number of SC pair counted: 0mM 3-MA, n=39; 1mM 3-MA, n=35; 2.5mM 3-MA, n=41; 5mM 3-MA, n=42. Statistical significance is determined by one-way ANOVA ($P > 0.05$, no significance) and the error bars show standard deviation (SD).

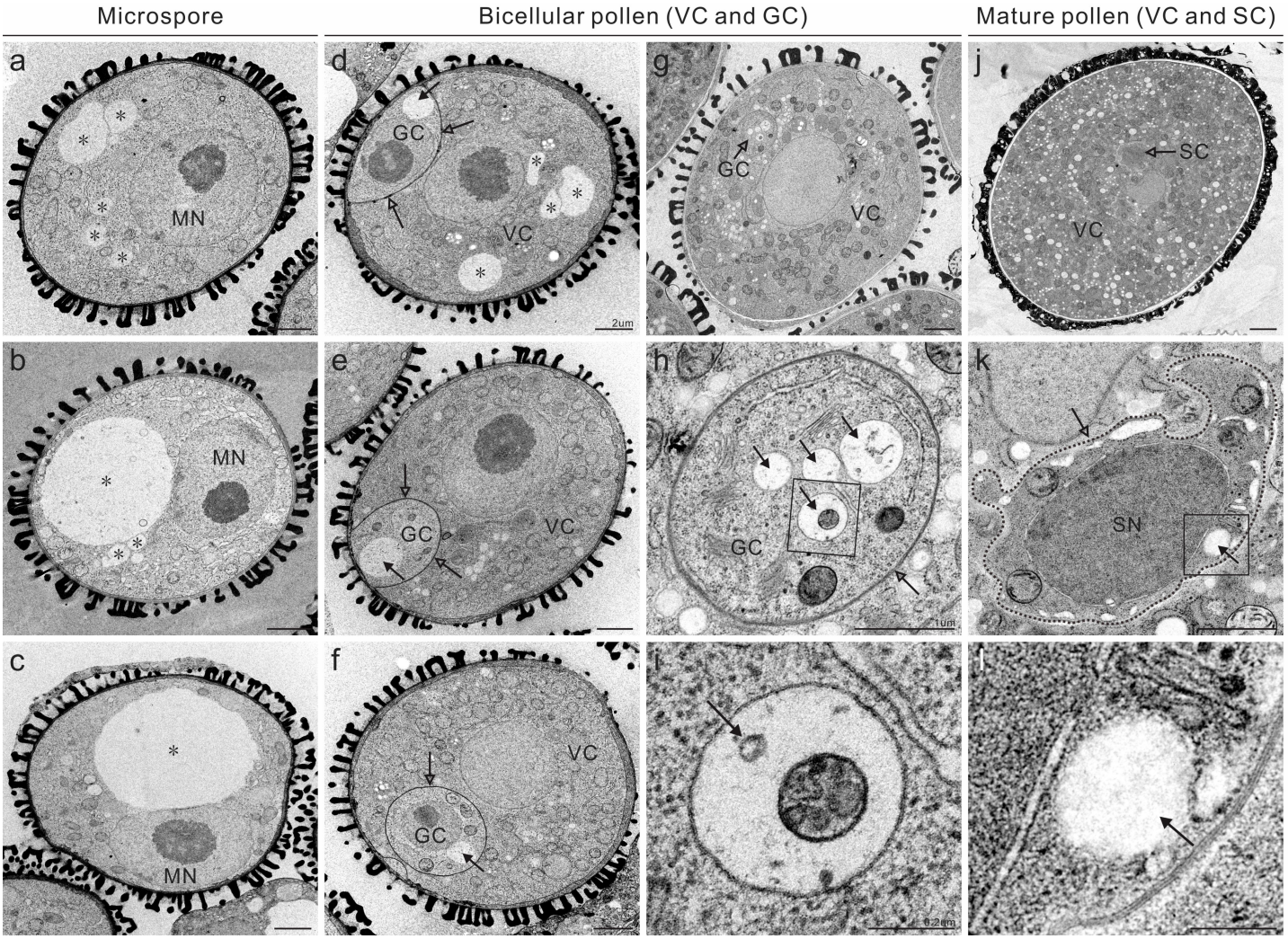

Extended Data Fig. 3 | Vacuolar dynamic during male gametogenesis in *A. thaliana*.

a-c, Vacuolar dynamic in microspore. Vacuoles are monolayer membrane structures with light osmic acid-staining, and are various in shape and size. Vacuoles are indicated by black asterisk (*). As the microspore nucleus moved peripherally to a position near the cell wall (**b** and **c**), a large central vacuole appeared, which was formed by the fusion of pre-existing small vacuoles. **d-i**, Vacuolar dynamic in bicellular pollen. After asymmetric microspore division, the large vacuole was again divided into small vacuoles (indicated by black filled arrows) which were assigned to both GC (indicated by black hollow arrows) and VC (**d**). Then, the vacuoles in VC became gradually undetectable, while those in GC were clearly visible (black filled arrows in **e-i**). **j-l**, Vacuolar dynamic in mature pollen. The spherical vacuoles (indicated by black filled arrows) existed uniquely in SC (indicated by black hollow arrows), while no longer clearly visible in VC at the mature pollen stage. The black dotted line indicated the SC membrane, which is distinguished between SC and VC. By identifying the plasma membrane (indicated by hollow arrows in **d**, **e**, **f**, **h**, **k**) and cell size, we can simply distinguish between germline cells (GC and SC) and the VC. In addition, VC contains specifically lipid bodies (tiny white dots in (**j**)), which are a monolayer membrane structure surrounded by the endoplasmic reticulum and are different from the vacuole; also see Extended Data Fig. 4b. Lipid bodies accumulate significantly in the mature pollen, so that GC and SC can be distinguished easily according to existence of lipid bodies. (**i** and **l**) The higher magnification view of the regions enclosed in the black boxes in (**h** and **k**). The conceivable degradation of paternal mitochondria displaying fragmentary bilayer membrane structure and cristae was observed in vacuoles within GC (**i**). Scale bars, 2μm (**a-e**, **g**, **h**, **j**, **k**, **n**), 0.5μm (**f**, **i**, **l**, **o**). MN, microspore nucleus; GC, generative cell; VC, vegetative cell; SC, sperm cell; SN, sperm cell nucleus.

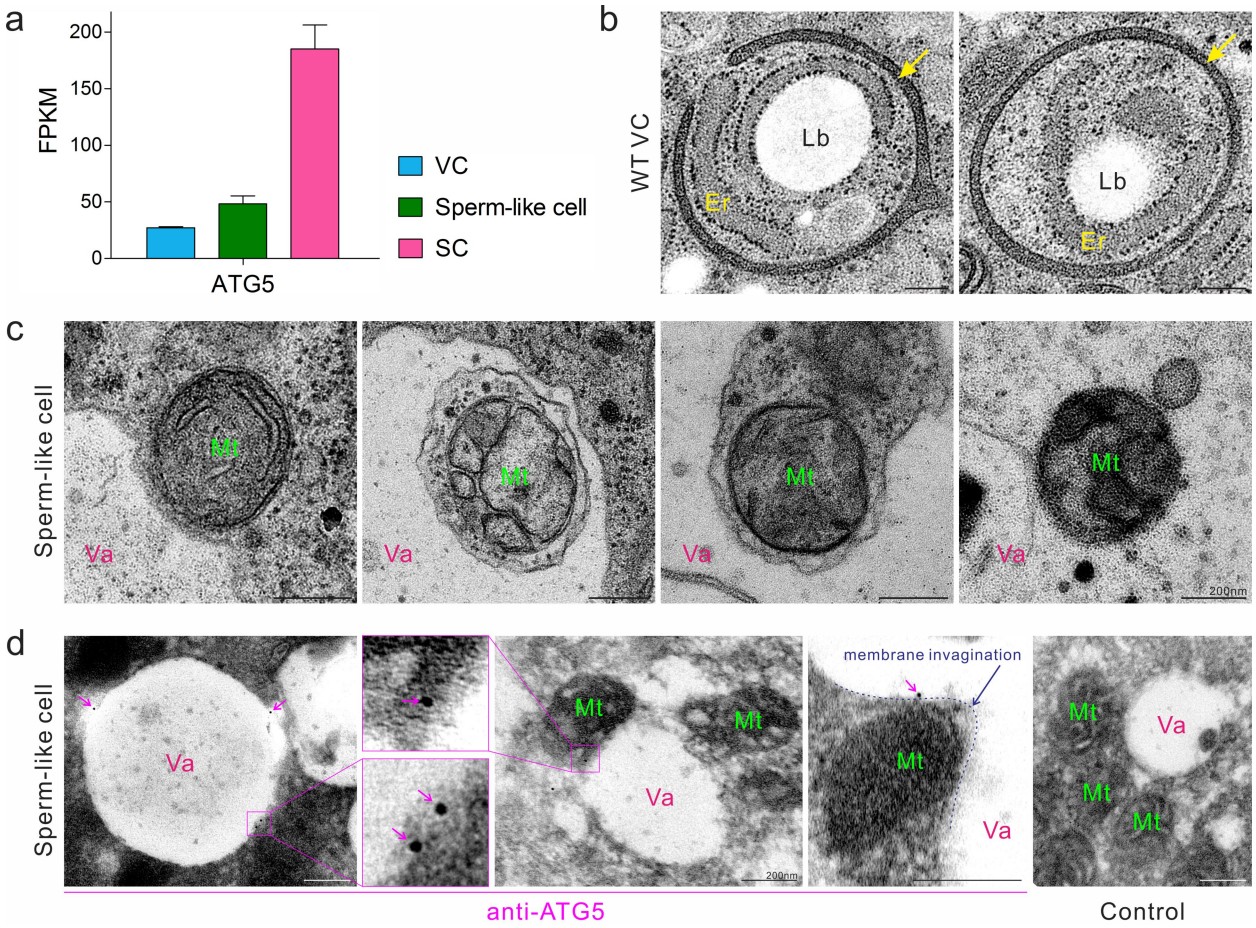

Extended Data Fig. 4 | The micromitophagy was activated in the *A. thaliana* sperm-like cell.

a, The transcript abundance of *ATG5*. *ATG5* was predominantly expressed in SC and increased as the developmental fate of VC shifted to male germline cells. **b**, Organelles degraded in VC via macroautophagy pathway. The growing phagophore wrapped VC-specific lipid body (left) and then formed an autophagosome structure (right). The arrows indicate phagophore (left) and autophagosome (right). **c**, Tomographic slice images of micromitophagy in the sperm-like cell. The corresponding 3D models are shown in Figure 4N. **d**, A vegetative to sperm cell fate switch system (Huang and Sun, 2022) allowed the monitoring of micromitophagy upon MG cell fate determination. Immuno-gold labeling with ATG5 antibody showed that in these sperm-like cells ATG5 localized to vacuole during the micromitophagy process. The magenta arrows, anti-ATG5 (10 nm gold particles). Scale bars, 200nm. VC, vegetative cell; SC, sperm cell; Va, vacuole; Lb, lipid body; Mt, mitochondrion; Er, endoplasmic reticulum.

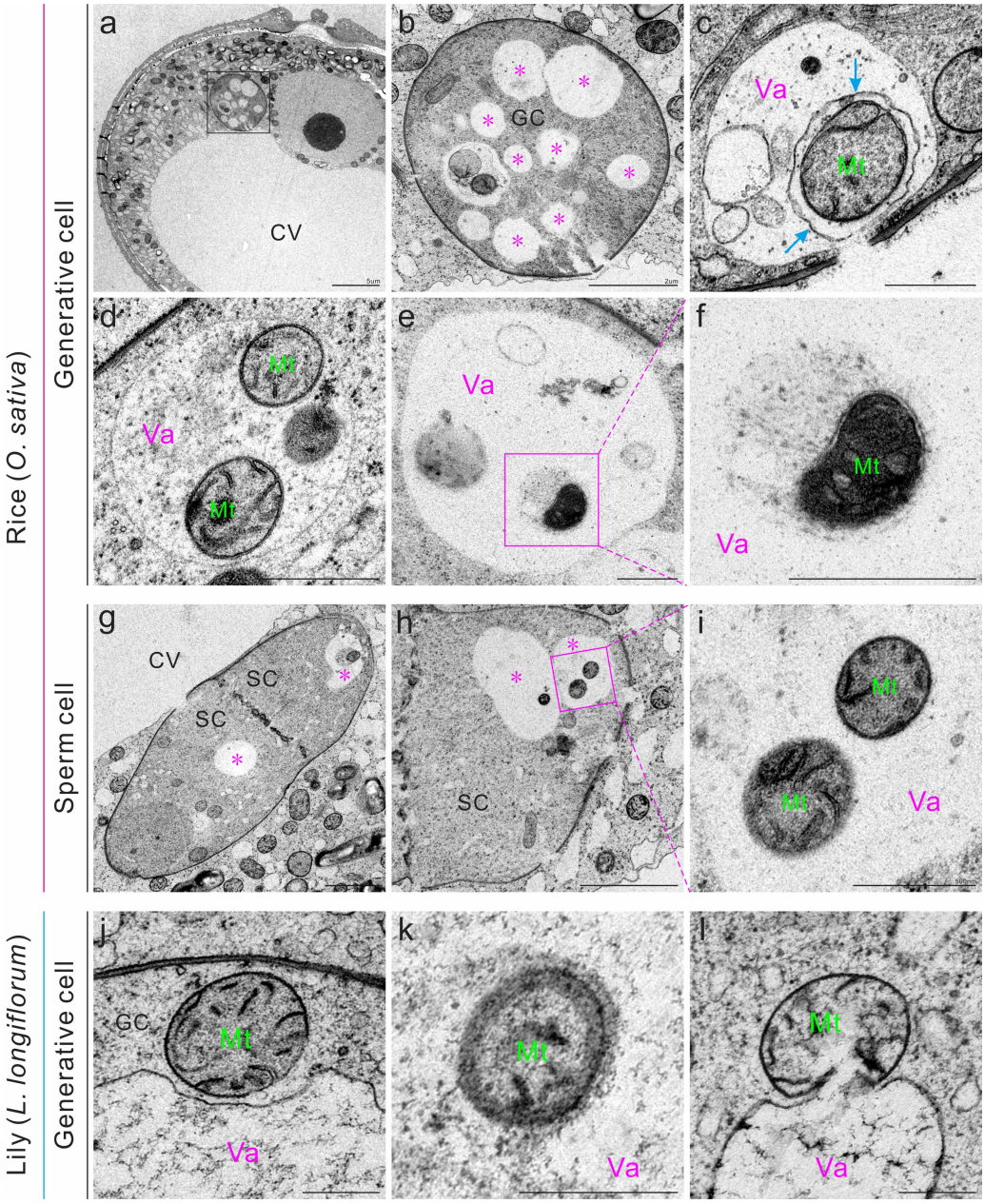

Extended Data Fig. 5 | Paternal micromitophagy during male gametogenesis in *O. sativa* and *L. longiflorum*.

a-l, The micromitophagy occurred in *O. sativa* GC (**a-f**) and SC (**g-i**). Mitochondria are labeled as Mt. There were many small dispersed vacuoles (indicated by the magenta asterisks (*) or labeled as Va) in GC and SC, but only one large central vacuole (CV) in VC. Micromitophagy occurred only in the small vacuoles (**c-f**, **h**, **i**), but not in the central vacuole (**a**, **g**). The trapped paternal mitochondria (PM) in a vacuole and formation of the micromitophagic vesicle (**c**). The blue arrows indicate the membrane of micromitophagic vesicles. Several mitochondria could be trapped in the same vacuoles (**d**, **h**, **i**). The micromitophagic vesicle with PM was degrading in the vacuole (**e**, **f**). (**f** and **i**) The higher magnification view of the regions enclosed in the dashed boxes in (**e** and **h**). **m-p**, The micromitophagy occurred in *L. longiflorum* GC. Type ①: the vacuole membrane invagination-mediated PM microautophagy was exhibited in *L. longiflorum* GC (**j**, **k**). (**k**) shows the degrading mitochondrion in the vacuole. Type ②: the micromitophagy mediated direct fusion of vacuole and PM in *L. longiflorum* GC (**l**). Scale bars, 5μm (**a**), 2μm (**b**, **g**, **h**), 500nm (**c-f**, **i-l**). GC, generative cell; SC, sperm cell; CV, central vacuole; Va, vacuole; Mt, Mitochondria.

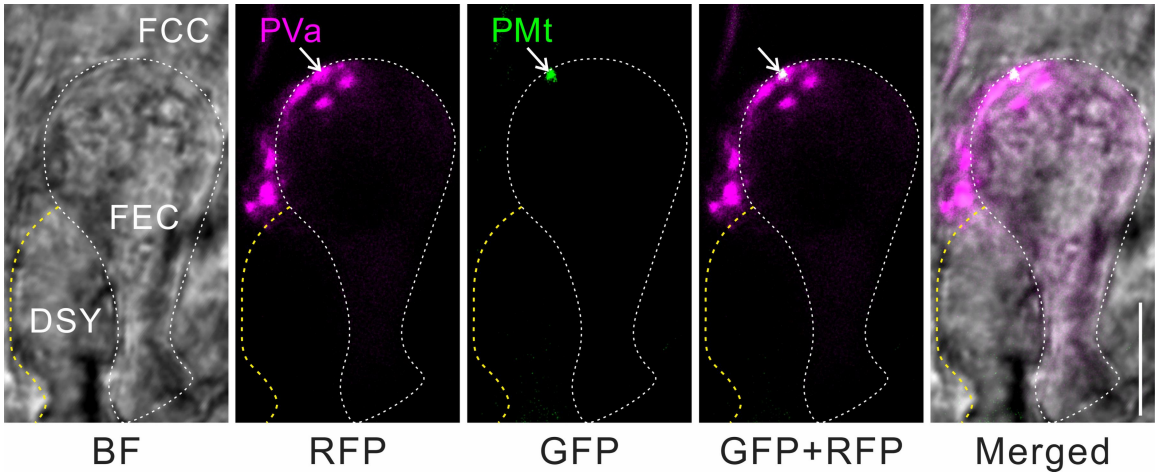

Extended Data Fig. 6 | The colocalization of paternal mitochondrion and vacuole in the fertilized egg cell.

Paternal mitochondrion (PMt) and vacuole (PVa) were able to colocalize in the fertilized egg cell (FEC). The *ProTIP5;1:TIP5;1-RFP ProDUO1:Mito-GFP* line (Two-marker line) were used as the paternal parent (♂), and WT was used as the maternal parent (♀). Scale bars, 10μm. DSY, degraded synergid cell; FCC, fertilized central cell.